

# Chapter 2

## Isoconversional Methodology

### 2.1 Evolution of Isoconversional Methods

*You must have accurate and honest weights and measures.*  
Deuteronomy 25:15

#### 2.1.1 Early Methods

The birth of isoconversional methods dates back to the 1925 work by Kujirai and Akahira [1]. In their work, they applied thermogravimetric analysis (TGA) data to follow the decomposition kinetics of some insulating materials under isothermal conditions. The mass loss data were fitted to an empirical equation

$$\log t = \frac{Q}{T} - F(w), \quad (2.1)$$

where  $w$  is the mass loss in percentage of the initial value,  $t$  is the time to reach the extent of decomposition  $w$  at different temperatures, and  $Q$  is what they called “material constant” that determines the temperature dependence of the decomposition rate. The  $Q$  values were estimated as a slope of  $\log t$  versus  $T^{-1}$  straight line.

It is not difficult to translate the meaning of  $Q$  and  $F(w)$  to modern kinetic language. Our basic kinetic equation can be written as:

$$\frac{d\alpha}{dt} = A \exp\left(\frac{-E}{RT}\right) f(\alpha). \quad (2.2)$$

Its integration for isothermal conditions yields:

$$g(\alpha) \equiv \int_0^\alpha \frac{d\alpha}{f(\alpha)} = A \exp\left(\frac{-E}{RT}\right) t, \quad (2.3)$$

where  $g(\alpha)$  is the integral form of the reaction model. Solving Eq. 2.3 for  $t$  and taking the decimal logarithm gives:

$$\log t = \frac{E}{2.303RT} - \log \left[ \frac{g(\alpha)}{A} \right]. \quad (2.4)$$

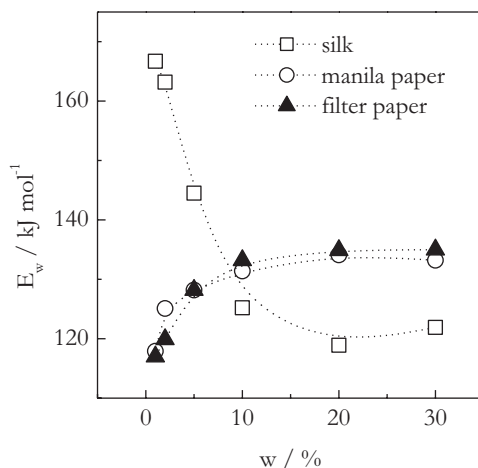
For any constant value of  $\alpha$ , the second term in Eq. 2.4 is constant and  $E$  can be determined from the slope of  $\log t$  versus  $T^{-1}$  without indentifying the form of the reaction model. As long as the total mass loss in percentage is independent of temperature, a constant value of  $w$  is equivalent to a constant value of  $\alpha$ . Then a comparison of Eq. 2.1 against Eq. 2.4 suggests that  $Q = E/2.303R$  and  $F(w) = \log[g(\alpha)/A]$ .

By using the method proposed by Kujirai and Akahira and their data, we can evaluate the activation energy as a function of mass loss,  $w$ . The resulting dependencies are shown in Fig. 2.1 [2]. It is worthy of note that the first ever isoconversional kinetic study reveals significant variations in the effective activation energy.

The work of Kujirai and Akahira did not seem to have much impact, so the method proposed by them was rediscovered by Dakin [3] in 1948. It appears to be of significance that in both papers the idea to bypass models in kinetic calculations came to mind of the workers who dealt with decomposition of complex materials, i.e., the materials that are nearly impossible to represent adequately by models. Nevertheless, isoconversional methods do not seem to have played any major role in isothermal kinetics, although sporadic examples of their use are found in monographic literature [4–7]. Isothermal kinetics appears to have always remained overwhelmingly focused on the model-fitting approach [8–10]. A rise of isoconversional methods to prominence is associated entirely with nonisothermal kinetics.

Since the early 1950s, commercially available thermal analysis instrumentation has been widely used to study thermal behavior of condensed-phase materials under nonisothermal conditions. This catalyzed intensive development of computational

**Fig. 2.1** The activation energies derived from data reported by Kujirai and Akahira [1]. (Reproduced from Vyazovkin [2] with permission of Taylor and Francis)



methods for evaluating nonisothermal kinetics. A comprehensive overview of the early methods is found in several books [11, 12]. The first isoconversional methods proposed for treatment of nonisothermal kinetics appeared nearly simultaneously in the 1960s. These were the differential method of Friedman [13] and the integral methods of Ozawa [14] as well as of Flynn and Wall [15, 16].

A simple rearrangement of Eq. 2.2 allows one to arrive at the equation of the Friedman method:

$$\ln \left( \frac{d\alpha}{dt} \right)_{\alpha,i} = \ln[f(\alpha) A_{\alpha}] - \frac{E_{\alpha}}{RT_{\alpha,i}}, \quad (2.5)$$

where the index  $i$  identifies an individual heating rate and  $T_{\alpha,i}$  is the temperature at which the extent of conversion  $\alpha$  is reached under  $i$ th heating rate. Then for any given  $\alpha$ , the value of  $E_{\alpha}$  is estimated from the slope of a plot of  $\ln(d\alpha/dt)_{\alpha,i}$  against  $1/T_{\alpha,i}$ . A great advantage of Eq. 2.5 is that it is applicable to not only linear heating program but also any temperature program at all. In particular, one can apply this equation to the actual sample temperature that may deviate from the preset non-isothermal or isothermal programs because the thermal effect of a process induces sample self-heating or self-cooling (see Sect. 1.3). The method is best applied to the data of differential type such as heat flow in differential scanning calorimetry (DSC). The application of the method to experimental data of the integral type such as mass loss data in TGA reveals an important disadvantage caused by the need of using numerical differentiation for estimating  $da/dt$ . The procedure dramatically amplifies the noise present in experimental data. For this reason, numerical differentiation has to be combined with smoothing. The latter must be performed with great care because it is known to introduce a systematic error (shift) in the smoothed data that would ultimately appear as a systematic error in the values of kinetic parameters.

The integral data are best treated by integral isoconversional methods that are derived from the integral form of Eq. 2.2:

$$g(\alpha) = A \int_0^t \exp\left(\frac{-E}{RT}\right) dt. \quad (2.6)$$

If the temperature is raised at a constant rate:

$$T = T_0 + \beta t, \quad (2.7)$$

where  $\beta$  is the heating rate; integration over time can be replaced with integration over temperature:

$$g(\alpha) = \frac{A}{\beta} \int_{T_0}^T \exp\left(\frac{-E}{RT}\right) dT \equiv \frac{A}{\beta} I(E, T), \quad (2.8)$$

where  $T_0$  is the initial temperature at  $t=0$  when the heating starts. The temperature integral,  $I(E, T)$ , has no analytical solution. It is solved either by replacing with one of numerous approximation functions [17] or by numerical integration. The traditional integral methods rely on the approximating functions,  $S(T)$ , that represent the integral value estimated within the integration limits from 0 to  $T$ , i.e.,

$$S(T) \approx \int_0^T \exp\left(\frac{-E}{RT}\right) dT. \quad (2.9)$$

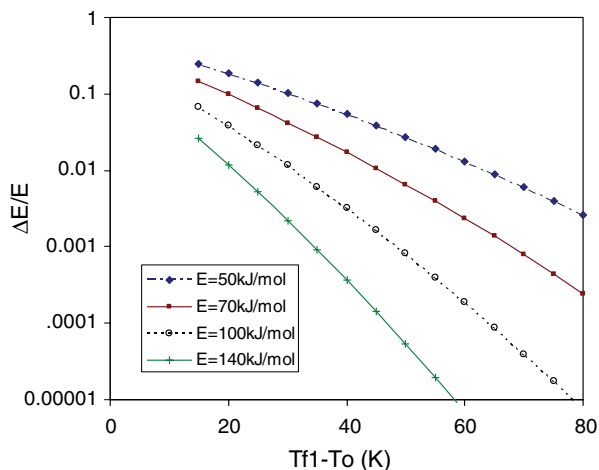
Then,  $I(E, T)$  in Eq. 2.8 should be equal to the difference in the values of the approximating functions estimated for the respectively different upper limits of integration,  $T$  and  $T_0$ :

$$I(E, T) \approx S(T) - S(T_0). \quad (2.10)$$

The traditional integral methods are derived by neglecting  $S(T_0)$ , i.e., the integral from 0 to  $T_0$ . This is equivalent to the assumption that the process rate between 0 and  $T_0$  is negligible. It is a reasonable assumption unless a process in question has low activation energy and becomes detectable at temperature close to the initial temperature. In such cases, neglecting the integral from 0 to  $T_0$  may introduce some error to the estimated value of  $E$ . The issue has been studied by Starink [18], and some of the results of that study are shown in Fig. 2.2. It is seen that as long as a process becomes detectable more than 50 °C above the initial temperature, the error in the estimated activation energy is likely to be negligible.

The Ozawa and Flynn and Wall methods were the first among a series of the traditional integral isoconversional methods. They both replace the temperature integral with a rather crude approximating function by Doyle [19]. The methods are represented by the same equation:

**Fig. 2.2** The relative error in the activation energy as a function of the activation energy and the distance between the initial temperature ( $T_0$ ) and temperature of a given conversion ( $T_f$ ) at the slowest heating rate  $\beta_1$ . (Reproduced from Starink [18] with permission of Springer)



$$\ln(\beta_i) = \text{Const} - 1.052 \left( \frac{E_\alpha}{RT_{\alpha,i}} \right), \quad (2.11)$$

where  $E_\alpha$  is estimated as a slope of the linear plot  $\ln(\beta_i)$  against  $1/T_{\alpha,i}$ . Repeating the procedure for a set of different  $\alpha$ 's gives rise to a dependence of  $E_\alpha$  on  $\alpha$ . Note that the integral methods can be also applied to the differential type of data that would have to be integrated numerically. Unlike numerical differentiation, integration does not amplify experimental noise that makes integral methods well suitable of either type of data.

It does not appear accidental that all three methods (i.e., Friedman, Ozawa, and Flynn and Wall) were proposed by workers who studied decomposition of complex polymeric materials, i.e., the processes for which finding an adequate kinetic model is more than challenging. It should be noted that the first applications of the methods immediately brought to light the issue of variable activation energy. Friedman [13] observed a variation in  $E_\alpha$  (Fig. 2.3) for decomposition of cured phenolic resin. Ozawa [14] found that  $E_\alpha$  varied for decomposition of both Nylon 6 and  $\text{CaC}_2\text{O}_4$  (Fig. 2.4). By using simulated data for competing and independent parallel reactions, Flynn [16] linked a variation in  $E_\alpha$  to the activation energies of the individual steps. This link has been explored systematically by Elder [20–23] and Dowdy [24, 25] for competing or independent reactions and by Vyazovkin for reactions complicated by diffusion [26], as well as for consecutive [27] and reversible reactions [28]. The studies have concluded that analysis of the  $E_\alpha$  can be used for obtaining some

**Fig. 2.3** The activation energies determined by Friedman for the thermal degradation of phenolic plastic. (Reproduced from Friedman [13] with permission of Wiley)

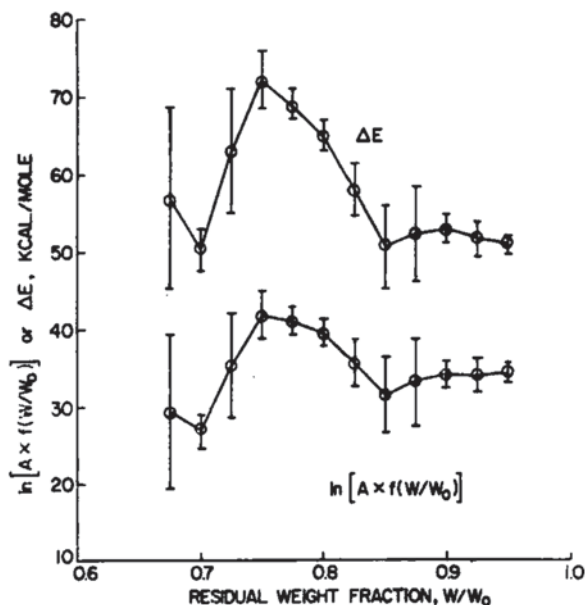
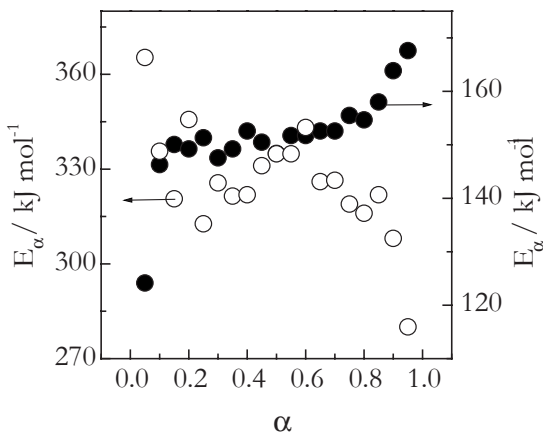


**Fig. 2.4** The activation energies reported by Ozawa [14] for the thermal decomposition of calcium oxalate (*open circles*) and Nylon 6 (*solid circles*)



clues about the reaction mechanisms as well as estimates of the activation energies of the individual steps [29].

As mentioned earlier, Eq. 2.11 is based on a very crude approximation of the temperature integral and, thus, should not be used without performing an iterative correction as described elsewhere [30, 31]. Alternatively, one can use isoconversional methods based on a more accurate approximation to the temperature integral. Starink [32] has demonstrated that many of these approximations give rise to linear equations of the general form:

$$\ln \left( \frac{\beta_i}{T_{\alpha,i}^B} \right) = \text{Const} - C \left( \frac{E_\alpha}{RT_{\alpha,i}} \right), \quad (2.12)$$

where  $B$  and  $C$  are the parameters determined by the type of the temperature integral approximation. For example, Doyle's approximation gives rise to  $B=0$  and  $C=1.052$  that turns Eq. 2.12 into Eq. 2.11 used by the methods of Ozawa and Flynn and Wall. A more accurate approximation by Murray and White gives rise to  $B=2$  and  $C=1$  and leads to another popular equation that is frequently called the Kissinger–Akahira–Sunose equation [33]:

$$\ln \left( \frac{\beta_i}{T_{\alpha,i}^2} \right) = \text{Const} - \frac{E_\alpha}{RT_{\alpha,i}}. \quad (2.13)$$

Relative to Eq. 2.11, Eq. 2.13 offers a significant improvement in the accuracy of the  $E_\alpha$  values. According to Starink [32], even more accurate estimates of  $E_\alpha$  can be accomplished when setting  $B=1.92$  and  $C=1.0008$  so that Eq. 2.12 takes the following form:

$$\ln \left( \frac{\beta_i}{T_{\alpha,i}^{1.92}} \right) = \text{Const} - 1.0008 \left( \frac{E_\alpha}{RT_{\alpha,i}} \right). \quad (2.14)$$

### 2.1.2 Modern Methods

Any further increase in the accuracy can be reached by means of isoconversional methods that compute the temperature integral as a part of evaluating  $E_\alpha$ . These methods can be referred to as flexible integral methods. By way of contrast, the traditional integral methods can be referred to as rigid integral methods. This is because in the latter integration was carried out as a part of deriving the final equation and thus cannot be modified. Several flexible isoconversional methods have been developed by Vyazovkin [34–36]. The methods employ the same numerical algorithm [34] that was developed under the basic isoconversional assumption that for any given  $\alpha$ ,  $g(\alpha)$  remains unchanged when changing the temperature program, e.g., the heating rate. Then, for  $n$  different heating rates, one can use the basic integral rate Eq. 2.8 to write the following equality:

$$g(\alpha) = \frac{A_\alpha}{\beta_1} I(E_\alpha, T_{\alpha,1}) = \frac{A_\alpha}{\beta_2} I(E_\alpha, T_{\alpha,2}) = \dots = \frac{A_\alpha}{\beta_n} I(E_\alpha, T_{\alpha,n}). \quad (2.15)$$

When the equality holds strictly, Eq. 2.15 is equivalent to

$$\sum_{i=1}^n \sum_{j \neq i}^n \frac{I(E_\alpha, T_{\alpha,i}) \beta_j}{I(E_\alpha, T_{\alpha,j}) \beta_i} = n(n-1). \quad (2.16)$$

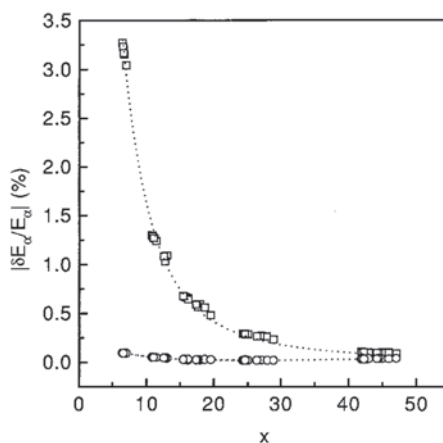
Since the values of  $T_\alpha$  are unavoidably measured with some error, the strict equality cannot be reached and the difference between left- and right-hand sides of Eq. 2.16 has to be minimized. The difference converges to a minimum when the left-hand side reaches a minimum. That is,  $E_\alpha$  is found as the value that secures a minimum of the following function:

$$\Phi(E_\alpha) = \sum_{i=1}^n \sum_{j \neq i}^n \frac{I(E_\alpha, T_{\alpha,i}) \beta_j}{I(E_\alpha, T_{\alpha,j}) \beta_i}. \quad (2.17)$$

The temperature integral in this equation is solved numerically or, for faster results, can be replaced with one of the highly accurate approximating functions [17] in accord with Eq. 2.10, i.e., without setting  $S(T_0)$  to 0. The minimization procedure is repeated for each value of  $\alpha$  to obtain a dependence of  $E_\alpha$  on  $\alpha$ .

A comparison of the relative errors in the activation energies estimated by Eqs. 2.17 and 2.13 (the method of Kissinger–Akahira–Sunose) indicates (Fig. 2.5) that the former is virtually error-free. On the other hand, the errors associated with the latter are practically negligible except when  $x = E/RT$  is very small, i.e., when a process occurs at high temperature and has unusually small activation energy. However, the major advantage of the proposed flexible method is that the user has total control over the process of integration and thus can modify it. In order to appreciate the value of such approach, one needs to realize that when using the traditional (i.e.,

**Fig. 2.5** Relative error in the activation energy as a function of  $x = E/RT$ ; nonlinear method, Eq. 2.16 (circles), linear Kissinger–Akahira–Sunose equation, Eq. 2.13 (squares). (Reproduced from Vyazovkin and Dollimore [34] with permission of ACS)



rigid) integral methods, the resulting activation energies are estimated in accord with a set of built-in assumptions. While maybe not obvious, these assumptions cannot be changed because they are a part of the final equation used for estimating the activation energy.

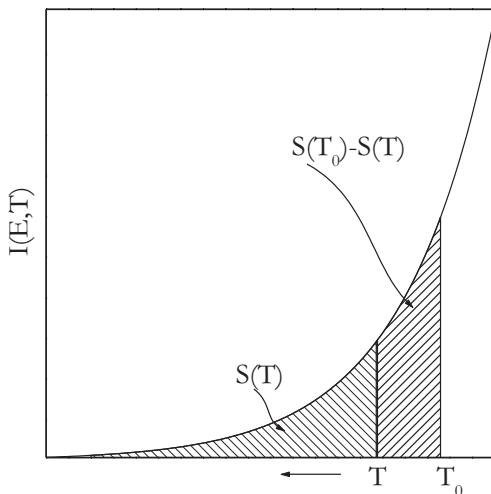
There are four built-in assumptions that affect the estimates of the activation energy determined with the rigid integral methods. The first one is using 0 instead of  $T_0$  for the lower integration limit in  $I(E, T)$  has already been mentioned. Since in a flexible method (e.g., Eq. 2.17) both integration limits are controlled by the user, one can perform integration from the actual value of  $T_0$ .

The second assumption is that the process occurs on heating making the traditional methods inapplicable to the processes that take place on cooling, such as crystallization. The heating-only assumption arises from the fact that  $I(E, T)$  is approximated as  $S(T)$  and not as the difference shown in Eq. 2.10. As cooling starts from the upper temperature  $T_0$  and  $T$  continuously decreases, the extent of conversion should increase in proportion to the increasing area  $S(T_0) - S(T)$  (Fig. 2.6). In the traditional integral methods, this area is approximated as  $S(T)$  and thus it would decrease with decreasing  $T$ . This is equivalent to a continuous decrease in the extent of conversion that obviously does not make sense. However, the area  $S(T_0) - S(T)$  can be determined correctly when using the flexible integral methods that make them suitable for treating a process that takes place on cooling.

The third built-in assumption is that the process temperature at any moment of time is determined entirely by the value of  $\beta$  (Eq. 2.7). In reality, the temperature estimated by Eq. 2.7 is the so-called reference temperature or simply the furnace temperature. The process temperature, though, is the sample temperature that can deviate from that of the reference due to either self-heating or self-cooling caused by the thermal effect of the process. Unless the deviations are negligible, one has to use the actual sample temperature in kinetic computations. The sample temperature can be used directly in the differential method such as that by Friedman (Eq. 2.5). However, it cannot be used in the integral methods whose equations include a single constant value of  $\beta$ . The fact that such value is included in the equation of an



**Fig. 2.6** For a process that takes place on cooling from  $T_0$  to  $T$ , the flexible methods estimate  $E_\alpha$  from the area  $S(T_0) - S(T)$  that corresponds to the actually accomplished extent of conversion. The rigid methods estimate  $E_\alpha$  from  $S(T)$  that represents the conversion, which is yet to be accomplished



integral method means that respective integration is performed assuming that the process temperature is equal to the furnace temperature. This issue can be resolved in a flexible integral method by replacing integration over temperature with integration over time. A specific method has been proposed by Vyazovkin [35]. In this method, the aforementioned algorithmic solution (Eqs. 2.15, 2.16 and 2.17) is adjusted to integration over time. The  $E_\alpha$  value is then determined by minimizing the following function [35]:

$$\Phi(E_\alpha) = \sum_{i=1}^n \sum_{j \neq i}^n \frac{J[E_\alpha, T_i(t_\alpha)]}{J[E_\alpha, T_j(t_\alpha)]}, \quad (2.18)$$

where  $J[E_\alpha, T(t_\alpha)]$  is defined as:

$$J[E_\alpha, T(t_\alpha)] = \int_0^{t_\alpha} \exp\left[\frac{-E_\alpha}{RT(t)}\right] dt \quad (2.19)$$

and  $T_i(t)$  is a set of arbitrary temperature programs. The integral is solved numerically and minimization is repeated for each value of  $\alpha$  to obtain a dependence of  $E_\alpha$  on  $\alpha$ . Equation 2.19 affords substitution of the actual sample temperatures for  $T(t)$ . The use of the actual sample temperature in Eq. 2.19 makes the method applicable to any preset program (i.e., isothermal as well as nonisothermal, be it linear or not) even if it is distorted by the thermal effect of the process.

The fourth built-in assumption is that at any  $\alpha$ , the value of  $E_\alpha$  is estimated as being constant in the whole range from 0 to  $\alpha$ . This again arises from the fact that the traditional rigid integral methods estimate the temperature integral in the form of Eq. 2.9, i.e., from 0 to  $T$ . As a result of such integration, the estimated  $E_\alpha$  values are strictly accurate only when  $E_\alpha$  does not vary with  $\alpha$ . Otherwise, the  $E_\alpha$  estimates

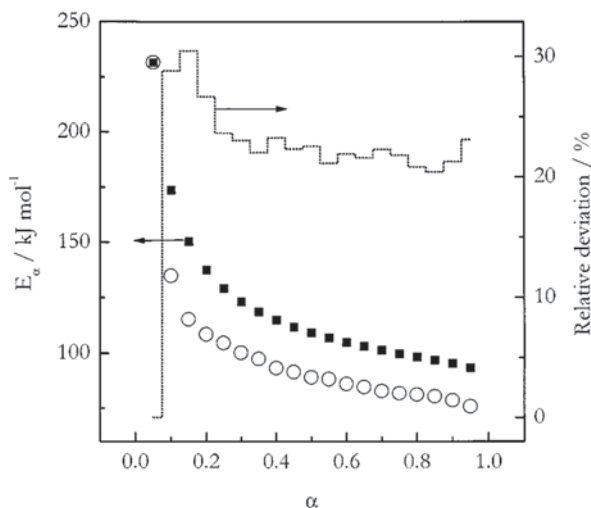
contain a systematic error whose size increases with increasing range of  $E_\alpha$  variability. The error can be eliminated by using a flexible integral method. All it takes is to perform either time or temperature integration by segments that correspond to small intervals of conversion,  $\Delta\alpha$ . Vyazovkin has proposed a method [36] that effectively eliminates this error by performing integration over small time segments. The method is based on Eq. 2.18, whereas Eq. 2.19 is modified as follows:

$$J[E_\alpha, T(t_\alpha)] = \int_{t_{\alpha-\Delta\alpha}}^{t_\alpha} \exp\left[\frac{-E_\alpha}{RT(t)}\right] dt. \quad (2.20)$$

When integration is carried out over small segments, the  $E_\alpha$  value is assumed to be constant only within a small interval of  $\Delta\alpha$  that is typically taken to be 0.01–0.02. The efficiency of integration by segments can be demonstrated by comparing the resulting  $E_\alpha$  versus  $\alpha$  dependence with that estimated by the Friedman method (Eq. 2.5). Because the latter is a differential method, it does not introduce the aforementioned integration error into the  $E_\alpha$  values. The application of the integral method with integration by segments and the differential Friedman method to the same set of simulated data demonstrates [36] that the resulting  $E_\alpha$  versus  $\alpha$  dependencies are virtually identical.

As already mentioned, in the integral methods, the systematic error introduced by non-constancy of  $E_\alpha$  is proportional to the magnitude of  $E_\alpha$  variation. In the case of significant variation of  $E_\alpha$  with  $\alpha$ , the relative error in  $E_\alpha$  can be as large as 20–30%. A process that is well known [2] to demonstrate significant variability of  $E_\alpha$  is the thermal dehydration of calcium oxalate monohydrate. The  $E_\alpha$  dependencies obtained by respectively neglecting and accounting for variability of  $E_\alpha$  are displayed in Fig. 2.7 which also shows the size of the error introduced when the variability is neglected. It is generally recommended [37] that one should account for variability

**Fig. 2.7**  $E_\alpha$  dependencies estimated for thermal dehydration of  $\text{CaC}_2\text{O}_4 \cdot \text{H}_2\text{O}$  by isoconversional method (Eq. 2.18). *Squares* represent the  $E_\alpha$  values obtained when using regular integration (Eq. 2.19). *Circles* represent the  $E_\alpha$  values estimated via integration by segments (Eq. 2.20). The *dotted line* shows the size of the relative error in  $E_\alpha$  caused by integration that does not account for variability of  $E_\alpha$ . (Reproduced from Vyazovkin [36] with permission of Wiley)



in  $E_\alpha$  when the difference between the maximum and minimum values of  $E_\alpha$  is more than 20–30% of the average  $E_\alpha$  value. In the case of calcium oxalate monohydrate, this difference is close to 100% of the average value.

Needless to say that performing integration over small temperature segments in accord with Eq. 2.21:

$$I(E_\alpha, T_\alpha) = \int_{T_{\alpha-\Delta\alpha}}^{T_\alpha} \exp\left(\frac{-E_\alpha}{RT}\right) dT \quad (2.21)$$

would also eliminate the error associated with the variability of  $E_\alpha$  in the isoconversional method based on Eq. 2.17. Consistency of the resulting  $E_\alpha$  dependence with the dependence produced by the Friedman method has been demonstrated by Budrugaec [38], who also proposed a new nonlinear differential isoconversional method that makes use of a numerical algorithm similar to that represented by Eqs. 2.15 and 2.16.

In addition to the methods proposed by Vyazovkin, there are several other flexible integral isoconversional methods [39–46]. Among them, a method proposed by Popescu [39] deserves a special attention because it combines the flexibility with computational simplicity. The method makes use of the so-called mean value theorem to approximate the temperature integral. The theorem states that a definite integral of a continuous function  $f(x)$  on the closed interval  $[a, b]$  can be presented as:

$$\int_a^b f(x) dx = (b-a)f(c), \quad (2.22)$$

where  $f(c)$  is the mean value of  $f(x)$  over the interval  $[a, b]$ . The equality is exact because the mean value is defined as:

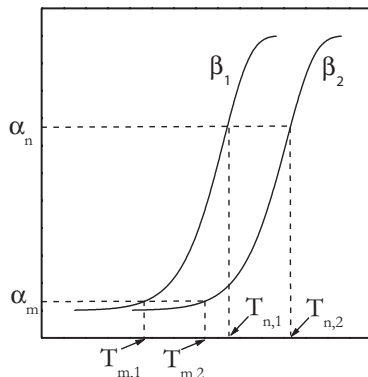
$$f(c) = \frac{1}{(b-a)} \int_a^b f(x) dx. \quad (2.23)$$

The theorem does not say where the point  $c$  is located, it only proves that it is located within the interval  $[a, b]$ . The application of the theorem to the temperature integral defined on the temperature interval  $[T_m, T_n]$  allows one to arrive at the following equation [39]:

$$\int_{T_m}^{T_n} \exp\left(\frac{-E}{RT}\right) dT = (T_n - T_m) \exp\left(\frac{-E}{RT_\xi}\right). \quad (2.24)$$

The equation is exact only when the value of  $T_\xi$  is such that the respective value of the exponential function equals the mean value of the function in the interval  $[T_m, T_n]$ . Unfortunately, there is no simple practical way to determine such tempera-

**Fig. 2.8** Illustration to the Popescu method (Eq. 2.26)



ture. For practical purposes, it can be approximated as the mean value of the interval  $[T_m, T_n]$ , i.e.,  $T_\xi = (T_m + T_n)/2$ . This approximation is accurate only for integration of a linear function. For any other function, the accuracy of this approximation would depend on the size of the interval  $[T_m, T_n]$  so that the smaller the interval, the better the accuracy. Subject to Eq. 2.24, one can write Eq. 2.8 for two arbitrary conversions  $\alpha_m$  and  $\alpha_n$ , as follows:

$$g(\alpha_n) - g(\alpha_m) = \frac{A}{\beta} (T_n - T_m) \exp\left(\frac{-E}{RT_\xi}\right), \quad (2.25)$$

where  $T_m$  and  $T_n$  are the temperatures that correspond, respectively, to the conversions  $\alpha_m$  and  $\alpha_n$  on the  $\alpha$  versus  $T$  curve at a given heating rate  $\beta$  (Fig. 2.8). Assuming that the form of the reaction model does not change with the heating rate, the left-hand side of Eq. 2.25 is constant for a set of different heating rates,  $\beta_i$ . Then Eq. 2.25 can be rearranged to:

$$\ln \frac{\beta_i}{T_{n,i} - T_{m,i}} = \text{Const} - \frac{E}{RT_{\xi,i}} \quad (2.26)$$

The activation energy can be determined from the slope of a linear plot of the left-hand side of Eq. 2.26 against  $1/T_{\xi,i}$ .

Although in the original publication [39] by Popescu, the intervals  $\Delta\alpha = \alpha_m - \alpha_n$  used are relatively wide (0.3–0.8), the relative errors in the estimated  $E$  values remain within the tenths of percent. However, the primary advantage of the method is in the flexibility to choose the integration limits by selecting any desired values of  $\alpha_m - \alpha_n$ . In particular, by making the  $\Delta\alpha$  intervals smaller (e.g., 0.01–0.02), one can practically eliminate the integration error that arises from the variability of  $E_\alpha$  with  $\alpha$ . This opportunity has been explored efficiently by Ortega [42], who applied the mean-value theorem to derive isoconversional equations for the conditions when

temperature increases linearly, stays constant, or changes nonlinearly. Figure 2.9 demonstrates the efficiency of the method as applied to a simulated process under conditions of linear heating. It is seen that approximating the temperature integral via the mean value theorem while keeping  $\Delta\alpha$  as small as 0.02 allows one to evaluate the correct  $E_a$  dependence. The accuracy of this method appears to be comparable to that of the methods proposed by Vyazovkin (Eqs. 2.18 and 2.20) and by Friedman (Eq. 2.5). Not surprisingly, the methods of Ozawa and Flynn and Wall (Eq. 2.11) as well as of Kissinger, Akahira, and Sunose (Eq. 2.13) cannot retrieve the correct  $E_a$  dependence because the integration used in these methods is not capable of accounting for variability of  $E_a$ .

Note that the equation derived by Ortega for linear heating conditions is similar to Eq. 2.26 obtained by Popescu, the only difference being that  $T_\xi$  is taken as  $T_{a'}$ , i.e., the upper limit of integration. The use of a single rather than averaged value of temperature as  $T_\xi$  can be a source of an unnecessary error as mentioned by Han et al., [47] who proposed to evaluate  $T_\xi$  as the mean of five temperatures from the interval  $T_{a-\Delta\alpha} - T_{a'}$ . This simple modification has been shown [47] to improve the accuracy of the method in the case of noisy simulated and actual experimental data.

All flexible integral isoconversional methods should in principle be applicable to treat processes that take place on cooling. This expands the application area of the methods to such processes as crystallization [48, 49], gelation [50], as well as some other phase transitions [51] that can be initiated by decreasing temperature. If a flexible method is based on integration with respect to temperature (e.g., Eq. 2.21 or 2.24), then under conditions of cooling, both temperature integral and heating rate

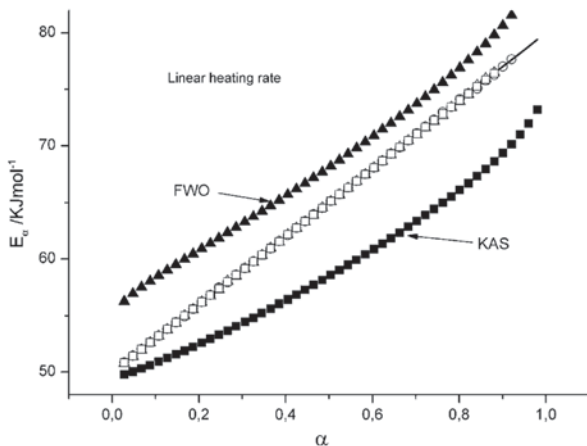
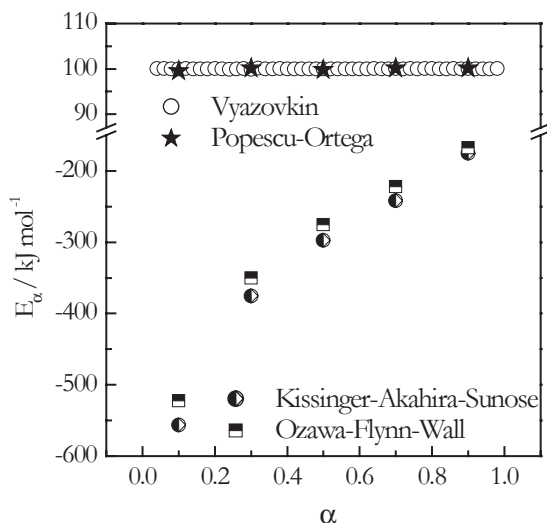


**Fig. 2.9** The process was simulated to have  $E_a$  to vary linearly with  $\alpha$ . Solid line represents the simulated  $E_a$  versus  $\alpha$  dependence. Open circles, triangles, and squares represent the  $E_a$  values estimated according to the methods proposed, respectively, by Ortega, Vyazovkin, and Friedman. All three methods yield the  $E_a$  values that coincide with the simulated ones. FWO and KAS represent the values estimated by the method of Flynn and Wall and Ozawa and by the method of Kissinger, Akahira, and Sunose. (Reproduced from Ortega [42] with permission of Elsevier)

**Fig. 2.10** The  $E_a$  values estimated by flexible (Vyazovkin, and Popescu and Ortega) and rigid (Ozawa and Flynn and Wall, and Kissinger and Akahira and Sunose) integral isoconversional methods. The size of the  $\Delta\alpha$  interval was taken to be 0.02 in both Vyazovkin and Popescu–Ortega methods



become negative so that  $g(\alpha)$  remains positive as it should (see Eq. 2.8). If integration is done with respect to time, the integral (Eq. 2.6) remains positive regardless of the direction in which temperature changes.

The appropriateness of the flexible integral methods for the processes occurring on cooling can be illustrated by applying two flexible integral methods to simulated data [52]. The data represent a process taking place on cooling with an activation energy 100 kJ mol<sup>-1</sup>. The methods selected are that proposed by Vyazovkin (Eqs. 2.18 and 2.20) and that proposed by Popescu and Ortega (Eq. 2.26). As seen from Fig. 2.10, both methods successfully retrieve the correct value of  $E$  from the cooling data. To reinforce the earlier made point that the rigid integral methods are not suitable for treating cooling data, we have applied the methods of Ozawa and Flynn and Wall as well as of Kissinger, Akahira, and Sunose to the same data set. These methods obviously produce erroneous values of the activation energy (Fig. 2.10). The failure is the direct consequence of the aforementioned (Fig. 2.6 and related discussion) inability of the rigid integral methods to properly evaluate the temperature integral on cooling.

As seen from the above brief overview, over a couple of past decades, isoconversional methods have developed into quite sophisticated computational tools capable of exploring thermally stimulated kinetics under a wide variety of temperature conditions. They have now become the most popular methods for kinetic analysis of the thermally stimulated processes. Per Scopus database, there are over two thousand papers that report the use of isoconversional methods over the last 4 years (2011–2014). However, the popularity of the methods started to grow quickly less than a decade ago. Apparently, the process was accelerated by the results of the 2000 Kinetic Project sponsored by the International Confederation for Thermal Analysis and Calorimetry (ICTAC) that once more highlighted critical deficiency of the single-heating-rate methods and vigorously emphasized [53–56] the necessity of abandoning them in favor of the methods based on multiple temperature programs.

It should be noted that single-heating-rate methods had dominated the field for decades, which was not very surprising. Given a choice, not many people would pick an isoconversional method that requires multiple runs in favor of a method that promises to produce the same information from just a single run. As a matter of fact, the need to perform more than a single run was considered [11] as a major disadvantage of isoconversional methods. The other point of critique typically was that isoconversional methods did not offer direct ways of determining the other two components of the kinetic triplet, i.e., the reaction model and preexponential factor. Computational techniques for estimating these two components are discussed in the next section.

## 2.2 Estimating Reaction Models and Preexponential Factors

*Tao creates the One.  
The One creates the Two.  
The Two creates the Three.  
The Three creates all things.*

Lao Tzu, Tao Te Ching: 42

### 2.2.1 Prelude

The ability of isoconversional methods to estimate the activation energy without estimating the reaction model has long been considered as one of their advantages. However, it is sometimes believed that the methods are not capable of estimating the reaction model as well as the preexponential factor. This is complete fallacy. As a matter of fact, the seminal paper [13] by Friedman describes not only the isoconversional method of estimating the activation energy but also a way of determining the preexponential factor and the reaction order model. Since then, some more sophisticated and accurate methods for estimating the preexponential factor and reaction model have been developed. Two very popular methods are discussed in this section.

Before we get to discussion of these methods, we need to forewarn one against some rather unsound approach to the problem that unfortunately is not quite uncommon. In it, the reaction model and preexponential factor are estimated by matching the activation energy estimated by an isoconversional method with the activation energy determined by some method that uses model fitting of single-heating-rate data. For example, one can fit  $d\alpha/dt$  versus  $T$  data obtained at one heating rate to Eq. 2.27

$$\ln \left( \frac{1}{f_j(\alpha)} \frac{d\alpha}{dt} \right) = \ln A_j - \frac{E_j}{RT}. \quad (2.27)$$

The equation is readily obtained by rearranging Eq. 2.2. The kinetic triplet is estimated by substituting some reaction model  $f_j(\alpha)$  in the left-hand side of Eq. 2.27 and fitting its dependence on the reciprocal temperature to a straight line. The intercept and slope of the line would, respectively, yield  $\ln A_j$  and  $-E_j/R$ . Such model-fitting results in obtaining as many kinetic triplets as the number of the reaction models one chooses to substitute in Eq. 2.27. Then, out of the multitude of obtained triplets, one picks a triplet whose  $E_j$  value matches best the activation energy value obtained by an isoconversional method. Such approach is unsound because of several methodological flaws. First, the  $E_j$  value frequently does not match the isoconversional activation energy with sufficient accuracy. Second, it is also not uncommon when more than one reaction model yields  $E_j$  values that match the isoconversional value within its confidence limits. Third, for the same reaction model, the  $E_j$  and  $A_j$  values commonly change with the heating rate. These factors introduce considerable inaccuracy in evaluation of the reaction models and preexponential factors.

On the other hand, the two methods discussed further afford accurate evaluation of the reaction model and preexponential factor subject to one important condition. The condition is that the process under study can be adequately represented by the single-step Eq. 2.2. This is readily verifiable by means of an isoconversional method. The condition is satisfied when the  $E_\alpha$  values do not demonstrate a systematic dependence on  $\alpha$  within a reasonably wide range of  $\alpha$ , e.g., 0.1–0.9. It is practically acceptable when the difference between the maximum and minimum values of  $E_\alpha$  is less than 10% of the average  $E_\alpha$  value. In the case of larger variability, the process cannot be considered as a single-step one. Any attempts to describe a multistep process by a single-reaction model and a value of the preexponential factor would give rise to inaccurate estimates of both.

## 2.2.2 The Use of the Compensation Effect

The first method we are going to discuss here allows one to employ the compensation effect for evaluation of the preexponential factor and the reaction model [29]. The method was originally proposed [57] for a single-step process. Later it was demonstrated [58] to work for estimating the preexponential factors of multistep processes. The method has been perfected by Sbirrazzuoli [59]. The compensation effect was already discussed briefly in Chap. 1 (Eq. 1.11). More detailed information is furnished elsewhere [60].

For the purpose of the present discussion, it would suffice to mention that the Arrhenius parameters  $\ln A_j$  and  $E_j$ , estimated by a single-heating-rate method (e.g., Eq. 2.27) are strongly correlated in the form of a linear relationship known as the compensation effect:

$$\ln A_j = aE_j + b, \quad (2.28)$$



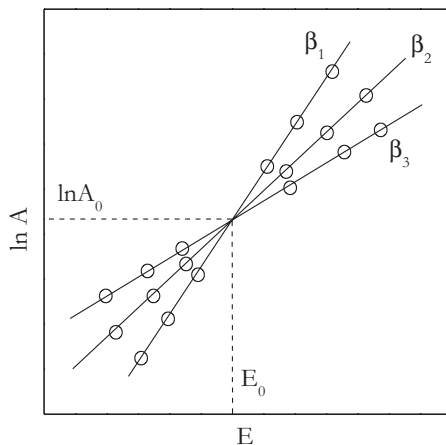
where  $a$  and  $b$  are the parameters of the compensation effect. The original work [57] by Vyazovkin and Lesnikovich has demonstrated two important properties of the compensation effect that are relevant to accurate evaluation of the preexponential factor. First, even if the correct model is not included in the list of models used to determine the  $\ln A_j$  and  $E_j$  values and if none of these values matches the correct values  $\ln A_0$  and  $E_0$ , the latter still lie on the compensation line determined by Eq. 2.28. This means that if the correct value of the activation energy is known, one can estimate the correct value of the preexponential factor by substituting  $E_0$  into Eq. 2.28. Second, although the parameters of the compensation effect depend on the heating rate, the latter does not affect the value of the preexponential factor estimated by substituting  $E_0$  into Eq. 2.28 obtained at different heating rates. The property arises from the fact [61] that the compensation lines related to different heating rates intersect at the points  $\ln A_0$  and  $E_0$  (Fig. 2.11). As a result, substitution of the correct value of the activation energy into the compensation line equation yields the same value of the preexponential factor regardless of the heating rate [57].

Overall, the method of estimating the preexponential factor boils down to the following four steps. First, an isoconversional method is applied to determine the activation energy,  $E_\alpha$ , as a function of conversion. Second, a single-heating-rate method is employed to determine several  $\ln A_j$  and  $E_j$  pairs. Third, the  $\ln A_j$  and  $E_j$  values are fitted to Eq. 2.28. Fourth, the  $E_\alpha$  values are substituted into Eq. 2.28 to yield the respective value of the preexponential factor:

$$\ln A_\alpha = aE_\alpha + b. \quad (2.29)$$

If  $E_\alpha$  is independent of  $\alpha$ , as one would expect for a single-step process, the resulting  $\ln A_\alpha$  is also invariable. Substitution of variable  $E_\alpha$  value obviously yields  $\ln A_\alpha$  value that depends on  $\alpha$ , which would be the case of a multistep process. As shown earlier [58], a dependence of  $\ln A_\alpha$  on  $\alpha$  can be used to estimate the preexponential factors of a multistep process. This has been recently reconfirmed by Sbirrazzuoli

**Fig. 2.11** Compensation lines  $\ln A_j = aE_j + b$  at three different heating rates  $\beta_1 < \beta_2 < \beta_3$ . The lines intersect at the correct values of the activation energy and preexponential factor. Circles represent the actual values of  $\ln A_j$  and  $E_j$  estimated by a single-heating-rate method (e.g., Eq. 2.27) while using different reaction models



[59], who also demonstrated that highly accurate values of the preexponential factor can be obtained when one evaluates the parameters of the compensation effect from only four pairs of  $A_j$  and  $E_i$  estimated by the single-heating-rate method of Tang et al. [62] when using the reaction models of Mampel (F1) and Avrami–Erofeev (A2, A3, A4).

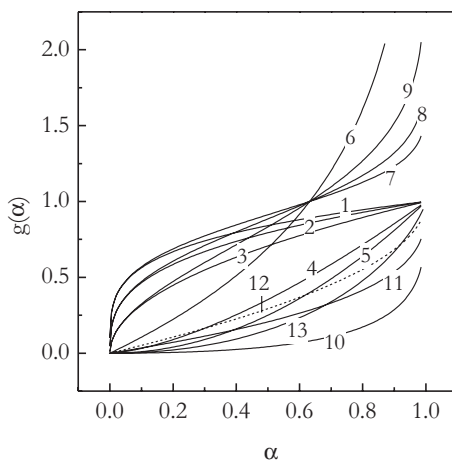
Once both  $E_\alpha$  and  $A_\alpha$  have been evaluated, it becomes possible to reconstruct numerically the reaction model in either integral or differential form [63]. The integral reaction model is reconstructed as follows:

$$g(\alpha) = \frac{A_\alpha}{\beta} \int_0^{T_\alpha} \exp\left(\frac{-E_\alpha}{RT}\right) dT. \quad (2.30)$$

Inserting in Eq. 2.30 the values of  $E_\alpha$ ,  $A_\alpha$ , and  $T_\alpha$  for each value of  $\alpha$  yields numerical values of  $g(\alpha)$  that can be matched to the theoretical  $g(\alpha)$  models (Fig. 2.12). In Eq. 2.30,  $T_\alpha$  is the experimentally measured temperature of reaching a certain  $\alpha$  at a given heating rate,  $\beta$ . However, the resulting values of  $g(\alpha)$  should not demonstrate any significant difference when using the  $T_\alpha$  values related to different heating rates. Note that the independence of the  $g(\alpha)$  dependences on  $\beta$  should be expected when  $E_\alpha$  (and thus  $A_\alpha$ ) are independent of  $\alpha$ , i.e., for a single-step process. As a matter of fact, accurate values of  $g(\alpha)$  can generally be evaluated when the process is a single-step one, because only in this case, the process can be described by a single-reaction model. When a process demonstrates significant variability of  $E_\alpha$ , its accurate description would require in general more than one kinetic triplet and in particular more than one reaction model. Nevertheless, analysis of the single  $g(\alpha)$  evaluated for a multistep process in some cases may provide useful insights [59].

Similar procedure and principles are applied when restoring the differential reaction model. The respective equation is obtained by rearranging Eq. 2.2 as follows:

**Fig. 2.12** Theoretical  $g(\alpha)$  dependencies. The numbers correspond to the model numbers from Table 1.1



$$f(\alpha) = \beta \left( \frac{d\alpha}{dT} \right)_\alpha \left[ A_\alpha \exp \left( \frac{-E_\alpha}{RT_\alpha} \right) \right]^{-1}, \quad (2.31)$$

where  $E_\alpha$  is estimated by an isoconversional method,  $A_\alpha$  is evaluated via the compensation effect, and  $T_\alpha$  and  $(d\alpha/dT)_\alpha$  are experimental values measured at the heating rate  $\beta$ . Substitution of the values into Eq. 2.31 yields numerical values of  $f(\alpha)$ , which can further be matched to the theoretical  $f(\alpha)$  models (Fig. 1.4).

Figures 2.13 and 2.14 exemplify the application of the aforementioned method in the case of thermal dehydration of nedocromil sodium trihydrate that occurs in two well-separated steps [64]. For both steps, the  $E_\alpha$  values estimated by an isoconversional method do not demonstrate practically any dependence of  $\alpha$  (Fig. 2.13). The compensation effect (Eq. 2.29) has been used to estimate the  $A_\alpha$  values, which were substituted in Eq. 2.30 to evaluate the reaction model,  $g(\alpha)$  in numerical form (points in Fig. 2.14). Comparison of the  $g(\alpha)$  values against the theoretical reaction models suggests that the first step of dehydration follows the zero-order reaction model,  $g(\alpha) = \alpha$  (R1).

However, for the second dehydration step, the  $g(\alpha)$  values fall between two diffusion models D2 and D3 (Table 1.1). This is not very unusual considering the

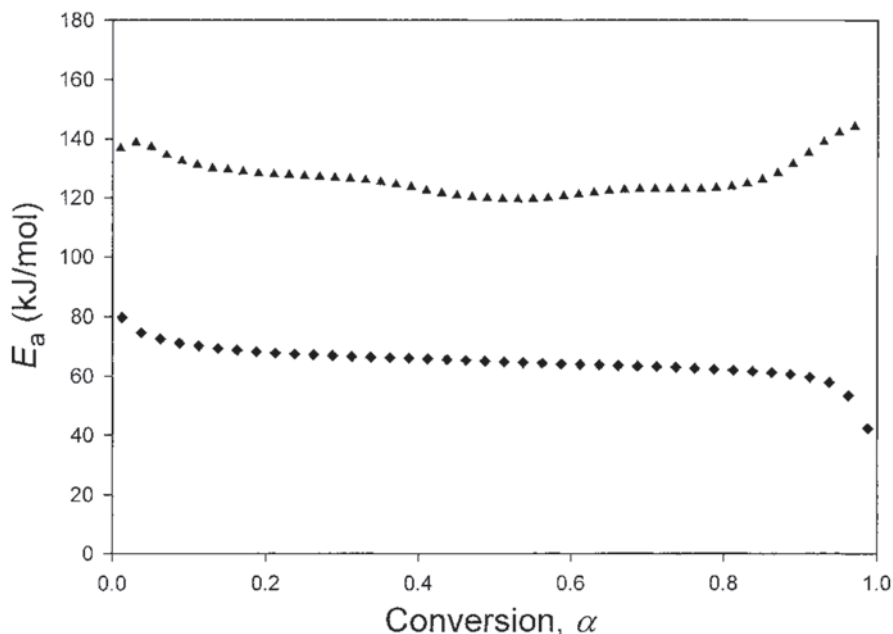


**Fig. 2.13**  $E_\alpha$  values estimated by an isoconversional method for first (diamonds) and second (triangles) steps of dehydration of nedocromil sodium trihydrate. (Reproduced from Zhu et al. [64] with permission of Wiley)

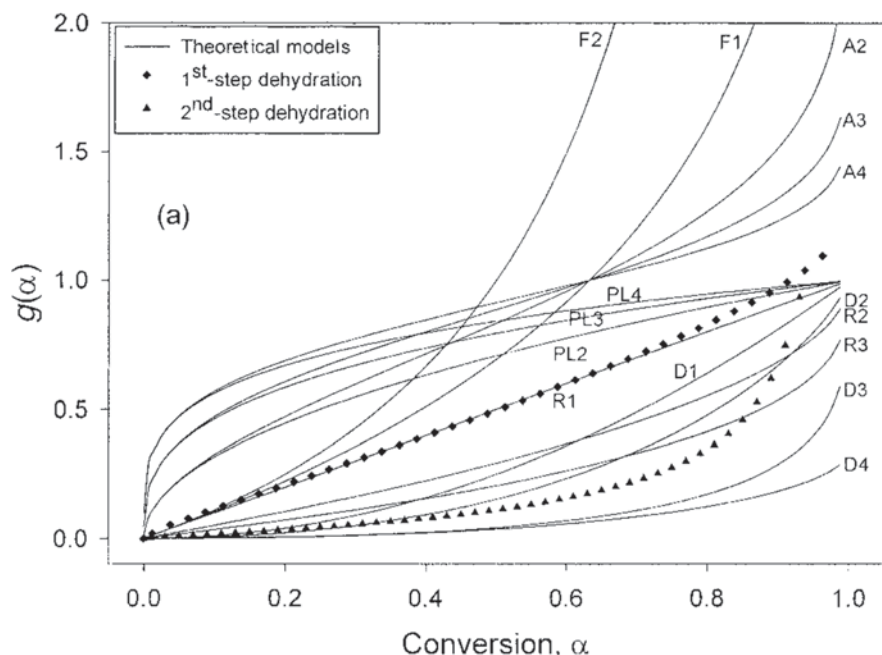


**Fig. 2.14** The  $g(\alpha)$  values estimated for the first (*diamonds*) and second (*triangles*) steps of dehydration of nedocromil sodium trihydrate. The solid lines represent the theoretical models. (Reproduced from Zhu et al. [64] with permission of Wiley)

following two problems. First, the selection of the models is always subjective and incomplete so that the proper model may simply be missing from the list. Second, the theoretical models were developed for largely idealized processes that often-times do not represent accurately the reality. For this reason, the theoretical reaction model is frequently used in the form with adjustable parameters, most popular being the so-called truncated Sestak–Berggren (SB) model [37]:

$$f(\alpha) = \alpha^m (1 - \alpha)^n. \quad (2.32)$$

Although this equation is frequently referred to simply as the SB model, the latter has one term more [65] than Eq. 2.32. On the other hand, Eq. 2.32 has been used in the heterogeneous kinetics years before [66, 67] the influential work [65] by Sestak and Berggren. A great advantage of Eq. 2.32 is that depending on the values of  $n$  and  $m$  it can imitate the three major types of kinetic curves, i.e., decelerating, accelerating, and sigmoid ones. Furthermore, Perez-Maqueda et al. have shown [68] that Eq. 2.32 can accurately match a number of theoretical models. The parameters  $n$  and  $m$  are easy to estimate by fitting the right-hand side of Eq. 2.32 to the numerical  $f(\alpha)$  values determined by Eq. 2.31. Unfortunately, the model does not exist in the integral form because the integral

$$g(\alpha) = \int_0^\alpha \frac{d\alpha}{\alpha^m (1-\alpha)^n} \quad (2.33)$$

does not have an analytical solution. However, the values of  $n$  and  $m$  can still be determined by fitting the right-hand side of Eq. 2.33 to the numerical values of  $g(\alpha)$  estimated by Eq. 2.30.

### 2.2.3 The Use of the $y(\alpha)$ or $z(\alpha)$ Master Plots

The use of the  $y(\alpha)$  or  $z(\alpha)$  master plots is another popular method of estimating the reaction models and preexponential factors. The method is contingent on  $E_\alpha$  being practically invariable with respect to  $\alpha$ . Therefore, as the first step in using this method, one needs to apply an isoconversional method for estimating  $E_\alpha$  as a function of  $\alpha$  and making sure that there is no significant variation. Then  $E_\alpha$  can be replaced with the mean value,  $E_0$ . The  $y(\alpha)$  function [69] has the following form:

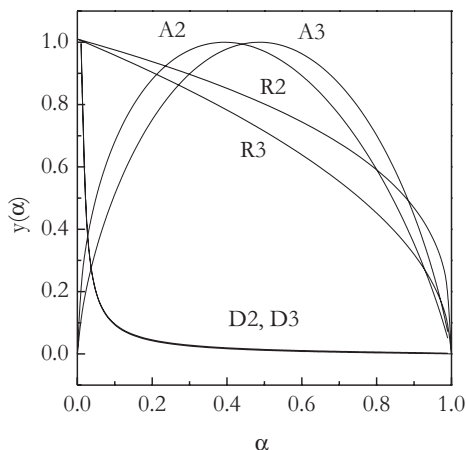
$$y(\alpha) = \left( \frac{d\alpha}{dt} \right)_\alpha \exp \left( \frac{E_0}{RT_\alpha} \right) = Af(\alpha). \quad (2.34)$$

Equation 2.34 is derived by rearranging Eq. 2.2. The values of  $y(\alpha)$  are calculated by using the experimental dependence of  $(d\alpha/dt)_\alpha$  on  $T_\alpha$  and multiplying it by the exponential term containing the  $E_0$  value estimated by an isoconversional method. The resulting numerical values of  $y(\alpha)$  are then plotted against  $\alpha$  and matched with the theoretical  $y(\alpha)$  master plots. The best match identifies a suitable model. Each heating rate gives rise to one experimental dependence of  $d\alpha/dt_\alpha$  on  $T_\alpha$  and, those, to one  $y(\alpha)$  plot. However, the resulting  $y(\alpha)$  plots should not demonstrate any significant variation with  $\beta$  producing a single  $y(\alpha)$  plot.

The fact that  $A$  is constant in 2.34 suggests that the shape of the  $y(\alpha)$  master plot is defined exclusively by the shape of the  $f(\alpha)$  functions (Fig. 1.4) that represent the differential form of the reaction model. Since the preexponential factor is yet to be estimated, the experimental and theoretical  $y(\alpha)$  plots are matched in a normalized form that sets their range of variation from 0 to 1. Examples of some normalized theoretical  $y(\alpha)$  plots derived from the  $f(\alpha)$  models (Table 1.1) are depicted in Fig. 2.15. The shape of the experimental  $y(\alpha)$  plot provides the first clue about the type of the reaction model. A convex decreasing dependence of  $y(\alpha)$  on  $\alpha$  is an indication of the contracting geometry models (coded R in Table 1.1). A concave decreasing plot is indicative of the diffusion models (code D). A dependence with a maximum is representative of either the Avrami–Erofeev (code A) or truncated SB models. The position of the maximum,  $\alpha_m$ , depends on the model (Table 2.1) that can help with identifying a particular one.

**Table 2.1** Values of  $\alpha_m$  and  $\alpha_p$  corresponding, respectively, to the maximum of the  $y(\alpha)$  and  $z(\alpha)$  functions for different kinetic models [37]

Kinetic model	$\alpha_m$	$\alpha_p$
R2	0	0.750
R3	0	0.704
F1	0	0.632
A2	0.393	0.632
A3	0.283	0.632
SB <sup>a</sup>	$m/(n+m)$	$\eta^b$
D2	0	0.834
D3	0	0.704

<sup>a</sup> SB stands for the truncated Sestak–Berggren equation (Eq. 2.32)<sup>b</sup> There is no general analytical solution for  $\alpha_p$ **Fig. 2.15** Some  $y(\alpha)$  plots built by normalizing the  $f(\alpha)$  functions of the respective reaction models (Table 1.1)

The  $z(\alpha)$  master plots are derived by combining the differential and integral forms of the reaction models. The temperature integral in Eq. 2.8 can be replaced with one of the multiple approximations [17],  $\pi(x)$ , as follows:

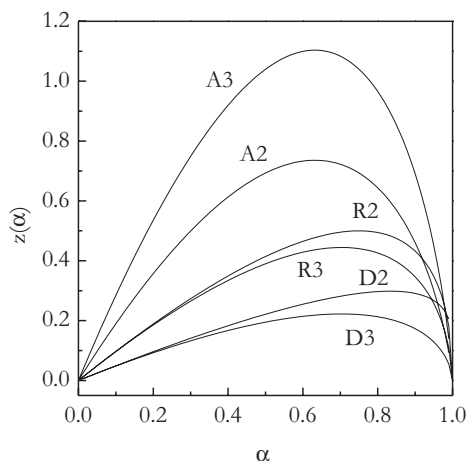
$$g(\alpha) = \frac{AE}{\beta R} \exp(-x) \left[ \frac{\pi(x)}{x} \right], \quad (2.35)$$

where  $x = E/RT$ . Combining Eqs. 2.35 and 2.2 and performing some rearrangements allow one to arrive at the  $z(\alpha)$  function as follows:

$$z(\alpha) = f(\alpha)g(\alpha) = \left( \frac{d\alpha}{dt} \right)_\alpha T_\alpha^2 \left[ \frac{\pi(x)}{\beta T_\alpha} \right]. \quad (2.36)$$

The last term in the brackets of Eq. 2.36 can be neglected [70] as it does not practically affect the shape of the  $z(\alpha)$  plot. Therefore, the  $z(\alpha)$  values can be calculated

**Fig. 2.16** Some  $z(\alpha)$  plots build as the product of  $g(\alpha)$  and  $f(\alpha)$  in accord with Eq. 2.36



by multiplying the experimental values of  $(d\alpha/dt)_\alpha$  by  $T_\alpha^2$ . The resulting experimental  $z(\alpha)$  values are plotted against  $\alpha$  and matched with the theoretical  $z(\alpha)$  master plots. The best match indicates an appropriate reaction model. As mentioned before, each heating rate produces one  $(d\alpha/dt)_\alpha$  versus  $T_\alpha$  dependence and thus one experimental  $z(\alpha)$  plot. However, all these plots should be nearly identical.

The theoretical  $z(\alpha)$  plots are obtained by plotting the product  $f(\alpha)g(\alpha)$  against  $\alpha$  for different reaction models. Figure 2.16 shows the theoretical  $z(\alpha)$  master plots for some of the models from Table 1.1. It is seen that all  $z(\alpha)$  plots pass through a maximum. Depending on the model, the  $z(\alpha)$  plots reach their maxima at specific values of conversion,  $\alpha_p$ , that are found from the condition [69]

$$g(\alpha)f'(\alpha) = -1. \quad (2.37)$$

The values of  $\alpha_p$  have been estimated [71] for a number of reaction models (Table 2.1). Comparing the maximum of the experimental  $z(\alpha)$  plot against the theoretical value (Table 2.1) provides the first clue about the type of the reaction model that might be applicable to the data.

Figures 2.17 and 2.18 provide an example of using the  $y(\alpha)$  and  $z(\alpha)$  plots to identify the reaction model for the thermal decomposition of nickel nitrate in air [72]. The use of the isoconversional methods demonstrates (Fig. 2.17) that the value of  $E_\alpha$  does not practically vary with  $\alpha$ . The experimental  $y(\alpha)$  and  $z(\alpha)$  plots are nearly identical and independent of the heating rate (Fig. 2.18). The presence of the maximum on the  $y(\alpha)$  plots suggests that an appropriate model should be either one of the Avrami–Erofeev or the truncated SB models. The experimental values of  $\alpha_m$  and  $\alpha_p$  were determined [72] to be smaller than those expected for the Avrami–Erofeev model (Table 2.1). For this reason, further analysis was based on the truncated SB model, for which the parameters  $m$  and  $n$  were estimated via model fitting.

Analysis of the  $y(\alpha)$  and  $z(\alpha)$  plots results in identification of the reaction model. The preexponential factor is estimated by the following equation [69]:

**Fig. 2.17** Activation energy determined by three different isoconversional methods for the thermal decomposition of nickel nitrate in air. (Reproduced from Jancovic et al. [72] with permission of Elsevier)

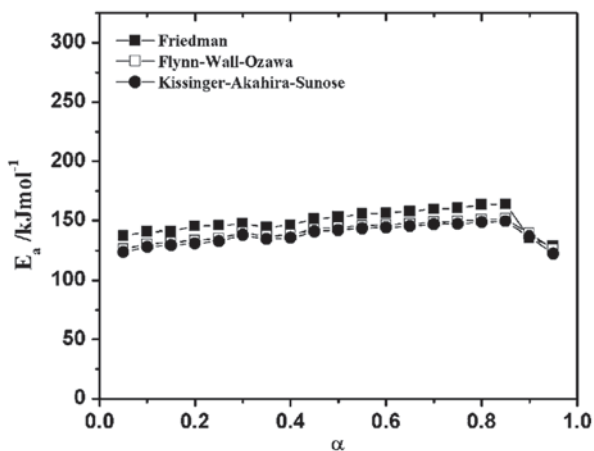
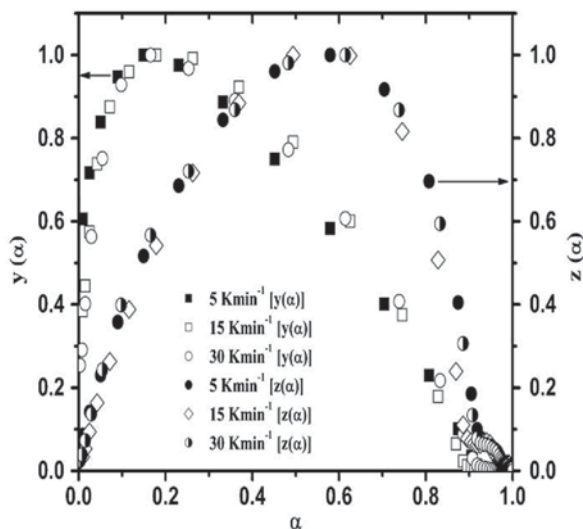


**Fig. 2.18** The  $y(\alpha)$  and  $z(\alpha)$  plots for the thermal decomposition of nickel nitrate in air. (Reproduced from Jancovic et al. [72] with permission of Elsevier)



$$A = \frac{-\beta E_0}{RT_{\max}^2 f'(\alpha_{\max})} \exp\left(\frac{E_0}{RT_{\max}}\right). \quad (2.38)$$

In Eq. 2.38, the subscript max denotes the values related to the maximum of the differential kinetic curve obtained at a given heating rate. That is,  $T_{\max}$  represents the peak temperature and  $\alpha_{\max}$  the extent of conversion at this temperature.



## 2.3 Kinetic Predictions

*But it had been one thing to foresee it mentally, and it was another to behold it actually.*

Henry James, *The Portrait of a Lady*

### 2.3.1 Why Predictions?

Kinetic predictions constitute the most important practical aspect of kinetic analysis. The essence of the latter is parameterization of the experimentally measured process rate as a function of such variables as the temperature, extent of conversion, and, sometimes, pressure. Parameterization means evaluating parameters of the equations (i.e., models) that represent a response of the process rate to a change in the aforementioned variables. Most commonly, one needs to parameterize the rate in terms of the temperature and conversion. This type of parameterization is accomplished by evaluating the kinetic triplet. Knowledge of a single kinetic triplet should be sufficient to predict the kinetics of a single-step process. Prediction of multistep kinetics would then require estimating multiple kinetic triplets, which is accomplished through model-fitting computations. However, isoconversional methods can be used to make adequate kinetic predictions for single- and multistep processes without estimating either preexponential factor or reaction model.

When it comes to kinetic predictions, one is typically interested in extrapolating some experimental kinetic measurements outside the actual temperature range, within which they were taken. The need in the extrapolations arises from practical difficulties of measuring the kinetics in the temperature range of interest. The actual measurements can be prohibitively difficult because the process is either too slow or too fast to measure by regular methods. Excessive costs as well as time limitations are among other practical factors that make one to choose predictions over actual measurements. A typical practical situation would be when one needs to select the most efficient stabilizer for a material that degrades slowly, e.g., on the scale of several years, at an ambient temperature. Measuring kinetics for several samples on such timescale would be unacceptably long and may require very expensive and sensitive equipment. A practicable alternative is to measure the kinetics at 40–50 °C above ambient temperature. This would accelerate the process and shorten its timescale from years to hours. Then, the higher-temperature kinetic data can be parameterized with respect to temperature and conversion, and the resulting parameters can be used to predict the kinetics at ambient temperature. The procedure is based naturally on the assumption that the kinetics would not change over the temperature range of extrapolation. In other words, it has to be assumed that the kinetic parameters estimated from higher temperature data should remain unchanged at ambient temperature. The same assumption allows one to make predictions from lower to higher temperature which is just as important. For instance, thermal stability of polymeric materials at

combustion temperatures can be predicted from experimental kinetic measurements conducted at significantly lower temperatures of thermal degradation.

Most commonly predicted parameter is the so-called lifetime. By its meaning, this is the time beyond which the material loses its properties to such degree that it cannot serve efficiently its intended purpose. For example, when exposed to heat, plastic polymeric material may lose plasticizer together with its plasticity. The methods of thermal analysis such as TGA and DSC are among the most common experimental techniques employed for estimating the lifetime of materials exposed to heat. As long as decay in the property of interest can be linked to a change in the mass or heat, the lifetime of a material can be estimated by the thermal analysis methods. TGA, for instance, can be readily used to measure the kinetics of plasticizer loss while exposing polymeric material to heating. Suppose that the critical decay of plasticity is reached when the material has lost 20 wt. % of plasticizer. Then, in kinetic terms, the initial state, when no plasticizer is lost, corresponds to the extent of conversion,  $\alpha=0$ . On continuous heating, the material would gradually lose 100 wt. % of plasticizer, reaching the final state ( $\alpha=1$ ). The critical state of the material would be reached at  $\alpha=0.2$ , i.e., at 20 wt.% loss of plasticizer. Then, the lifetime of the material can be estimated as the time to reach  $\alpha=0.2$ , i.e.,  $t_{0.2}$ . Let us consider several methods of estimating (predicting) the time to reach a given extent of conversion,  $t_\alpha$ .

### 2.3.2 Model Based Versus Model Free

For a single-step process taking place at constant temperature,  $T_0$ , the time to reach any given value of  $\alpha$  is readily determined by rearranging Eq. 2.3:

$$t_\alpha = \frac{g(\alpha)}{A \exp\left(\frac{-E}{RT_0}\right)}. \quad (2.39)$$

Equation 2.39 affords prediction of the lifetime of material exposed to isothermal heating at the temperature  $T_0$ . To employ this equation, one needs to evaluate the whole kinetic triplet for the process responsible for the decay in the property of interest. For example, in the aforementioned case of the polymeric material losing its plasticity, this process is the mass loss of the plasticizer. The triplet can be evaluated from isothermal as well as nonisothermal experiments. However, one should be warned specifically against using single-heating-rate methods. These methods produce notoriously unreliable kinetic triplets that give rise to meaningless kinetic predictions [73].

Equation 2.39 provides a foundation for two American Society for Testing and Materials (ASTM) methods developed for evaluating the thermal stability from TGA (E1641 [74]) and DSC (E698 [75]) data. The predictive equation utilized by E1641 is:

$$t_\alpha = \frac{-\ln(1-\alpha)}{A \exp\left(\frac{-E}{RT_0}\right)}, \quad (2.40)$$

where the value of  $E$  is estimated by the Flynn and Wall method (Eq. 2.11). Comparison of Eqs. 2.40 and 2.39 suggests that  $g(\alpha) = -\ln(1-\alpha)$ , which means that Eq. 2.40 is based on the assumption that the process obeys first-order kinetics (Table 1.1). This assumption is also used to estimate the preexponential factor in Eq. 2.41:

$$A = \frac{\bar{\beta} R}{E_r} \ln(1-\alpha) 10^a, \quad (2.41)$$

where  $\bar{\beta}$  is the mean of the experimental heating rates used to determine  $E$  by the Flynn and Wall method (Eq. 2.11). The  $E_r$  value is the corrected value of the activation energy. It is determined by dividing the experimental value of  $E$  by the correction factor that compensates for the inaccuracy of Doyle's approximation of the temperature integral. The ASTM document [74] lists the values of both the correction factor and the parameter  $a$  in Eq. 2.41.

The predictive equation utilized by E698 is the same as the one used by E1641 (Eq. 2.40). The value of  $E$  is recommended to be estimated either by the method of Kissinger [76, 77] or by the methods of Ozawa and Flynn and Wall (Eq. 2.11). In the latter case, the ASTM document [75] recommends replacing  $T_\alpha$  in Eq. 2.11 with the peak temperature,  $T_p$ . Just as E1641, the E698 method makes the assumption of the first-order kinetics in its predictive equation and in the equation for estimating the preexponential factor:

$$A = \frac{\beta E}{RT_p^2} \exp\left(\frac{E}{RT_p}\right). \quad (2.42)$$

The major shortcoming of both ASTM methods is that the lifetime is predicted by assuming the first-order kinetics as well as the constancy of the activation energy. If any of these assumptions does not hold, the prediction would be in error. Figure 2.19 demonstrates a considerable deviation of the ASTM prediction from the experimental data on the thermal degradation of poly(ethylene 2,6-naphthalate) (PEN), the process that demonstrates a significant variation of  $E_\alpha$  with  $\alpha$  [78]. More examples of similar problems with the ASTM predictions are found elsewhere [73, 79]. Therefore, before using the ASTM methods, one should be advised to check whether  $E_\alpha$  does not vary significantly with  $\alpha$  and whether the reaction model is that of first order.

The shortcomings of the ASTM methods are circumvented by employing the model-free predictions. The latter utilize the dependence of  $E_\alpha$  on  $\alpha$  evaluated by an

isoconversional method. Originally, the model-free predictive equation was derived [29, 80] in the following form:

$$t_{\alpha} = \frac{\int_0^{T_{\alpha}} \exp\left(\frac{-E_{\alpha}}{RT}\right) dT}{\beta \exp\left(\frac{-E_{\alpha}}{RT_0}\right)}. \quad (2.43)$$

This equation is derived by equating the right-hand sides of Eqs. 2.3 and 2.8 and cancelling the  $A$  values. This action is justified by the aforementioned assumption that the kinetic triplet does not change over the temperature range of extrapolation. There is an important methodological difference between Eqs. 2.43 and 2.39. The latter does not directly use any experimentally measured kinetic curves to make the predictions. The kinetic curves are replaced with the kinetic triplet. On the other hand, Eq. 2.43 makes use of the kinetic curve  $\alpha$  versus  $T$  measured at certain heating rate  $\beta$ . In other words, Eq. 2.43 is a way of converting actually measured nonisothermal kinetic data into isothermal data expected at a given temperature  $T_0$ . Since several heating rates are used to evaluate the  $E_{\alpha}$  dependence, any of the respective  $\alpha$  versus  $T$  curves can be used for making predictions by Eq. 2.43. In theory, there should be no significant difference between the lifetimes predicted when using the  $\alpha$  versus  $T$  curves obtained at different  $\beta$ . This is because the numerator of Eq. 2.43 divided over  $\beta$  is  $g(\alpha)$ , whose value is constant at  $\alpha = \text{const}$  for all heating rates involved. In practice, the lifetime predicted from different heating rates can demonstrate some variability that is reduced by replacing the respective  $t_{\alpha}$  values with the mean or median value.

Since Eq. 2.43 performs integration from 0 to  $T_{\alpha}$ , assuming that  $E_{\alpha}$  remains constant from 0 to  $\alpha$ , it cannot properly account for variability of the activation energy with the extent of conversion. As mentioned earlier, this can lead to significant systematic errors in the case of a strong variation of  $E_{\alpha}$  with  $\alpha$ . For this reason, the original Eq. 2.43 was later [81] modified to account for such variations. The latter are accounted properly when performing integration by small segments (see Eq. 2.21). Then, if the interval from 0 to  $\alpha$  is split in  $k$  segments, Eq. 2.43 can be used to predict time for each individual segment:

$$t_{\alpha,i} = \frac{\int_{T_{\alpha,i-1}}^{T_{\alpha,i}} \exp\left(\frac{-E_{\alpha,i}}{RT}\right) dT}{\beta \exp\left(\frac{-E_{\alpha,i}}{RT_0}\right)}. \quad (2.44)$$

Then, the total time to reach  $\alpha$  will be the sum of the times for all  $k$  segments:

$$t_\alpha = \sum_{i=1}^k t_{\alpha,i} = \frac{1}{\beta} \sum_{i=1}^k \frac{I(E_{\alpha,i}, T_{\alpha,i})}{\exp\left(\frac{-E_{\alpha,i}}{RT_0}\right)}. \quad (2.45)$$

The resulting Eq. 2.45 allows one to use nonisothermal constant heating-rate experiments to predict the isothermal lifetimes while properly accounting for variation of  $E_\alpha$  with  $\alpha$ . Similarly, the isothermal lifetimes can be predicted from data obtained under arbitrary temperature programs,  $T(t)$ . The respective equation is as follows:

$$t_\alpha = \sum_{i=1}^k t_{\alpha,i} = \sum_{i=1}^k \frac{J[E_{\alpha,i}, T[(t_{\alpha,i})]]}{\exp\left(\frac{-E_{\alpha,i}}{RT_0}\right)}, \quad (2.46)$$

where  $t_{\alpha,i}$  is calculated as [81]

$$t_{\alpha,i} = \frac{\int_{t_{\alpha,i-1}^*}^{t_{\alpha,i}^*} \exp\left[\frac{-E_{\alpha,i}}{RT(t)}\right] dt}{\exp\left(\frac{-E_{\alpha,i}}{RT_0}\right)}. \quad (2.47)$$

In Eq. 2.47,  $t_\alpha^*$  is the experimentally estimated time to reach a given value of  $\alpha$  under the temperature program,  $T(t) = T^*(t)$ . This is one of the several temperature programs employed for evaluating the  $E_\alpha$  dependence.

The predictions made by Eqs. 2.43, 2.45, and 2.46 can be called “model-free predictions,” because they get rid of the reaction model  $g(\alpha)$  in the numerator of Eq. 2.39. The most important feature of the model-free predictions is that each value of  $t_\alpha$  is predicted by using the corresponding value of  $E_\alpha$ . In other words, the model-free predictive equations allow for using the actual  $E_\alpha$  dependence. This expands the application area of these equations to both single-step ( $E_\alpha$  does not depend on  $\alpha$ ) and multistep ( $E_\alpha$  depends on  $\alpha$ ) processes. The model-free predictions provide two obvious advantages over the ASTM methods. First, they are not limited to the first-order kinetics or any other reaction model. Second, they do not require  $E_\alpha$  to be invariable with  $\alpha$ . For this reason, they generally give rise to more reliable kinetic predictions than the ASTM methods. This fact is exemplified in Fig. 2.19 and elsewhere [73, 79].

Although most commonly one makes predictions of the lifetime at a given constant temperature,  $T_0$ , by using a set of nonisothermal measurements, the kinetic predictions can be made from kinetic data measured at temperature programs  $T^*(t)$  to any temperature program of interest,  $T_0(t)$ . Using the same assumption as in deriving Eq. 2.43, one can arrive at a model-free equation:

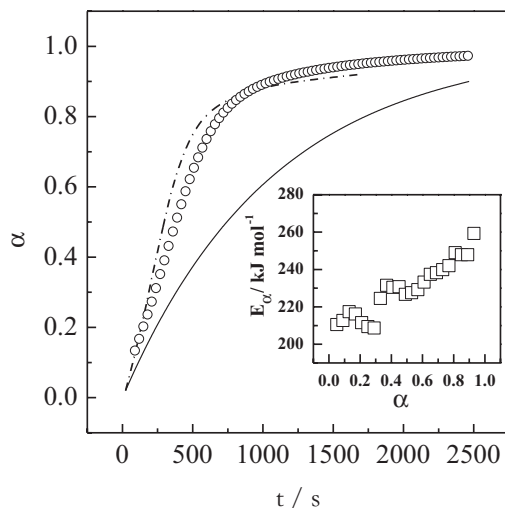


**Fig. 2.19** ASTM E1641 (solid line) and model-free (dash-dot line) predictions of the thermal degradation of PEN in nitrogen at 420 °C compared to the actually measured data (circles, the initial portion is not shown to avoid overcrowding). Inset shows the  $E_\alpha$  dependence evaluated by an isoconversional method from nonisothermal TGA data. (Reproduced from Prime et al. [78] with permission of Wiley.) ASTM American Society for Testing and Materials, PEN poly(ethylene 2,6-naphthalate)

$$J[E_\alpha, T_0(t_\alpha)] = J[E_\alpha, T^*(t_\alpha^*)]. \quad (2.48)$$

In Eq. 2.48, the right-hand side represents the integral (Eq. 2.21) over a particular experimental temperature program,  $T^*(t)$ . Then the lifetime  $t_\alpha$  at any desired temperature program  $T_0(t)$  is estimated as a numerical solution of Eq. 2.48.

### 2.3.3 Understanding Precision and Accuracy of Predictions

It is important to keep in mind that any kinetic prediction has its inherent limits in terms of precision and accuracy. Unavoidable noise in experimental measurements (i.e.,  $T$ ,  $\alpha$ ,  $da/dt$ ) leads to random errors in estimating the kinetic triplet. These random errors further propagate into the error of the lifetime value. For example, the relative error in the lifetime predicted by Eq. 2.43 is estimated [82] approximately to be

$$\left| \frac{\Delta t_\alpha}{t_\alpha} \right| \approx \left| \Delta E_\alpha \left( \frac{1}{RT_0} - \frac{1}{RT_\alpha} - \frac{1}{E_\alpha} \right) \right|. \quad (2.49)$$

This equation suggests that as the temperature of prediction,  $T_0$ , moves further away from the experimental temperature,  $T_\alpha$ , the relative error in the lifetime increases

and should at certain point exceed 1, i.e., 100%. This means that the absolute error  $\Delta t_\alpha$  would exceed the  $t_\alpha$  value itself that deems the prediction meaningless. For example, if  $E_\alpha = 200 \pm 10 \text{ kJ mol}^{-1}$  and  $T_\alpha = 400 \text{ K}$ , the 100% error is reached when predicting to  $T_0 = 297 \text{ K}$ . Although the error in the lifetime depends on the parameters of Eq. 2.49, the obtained estimate gives a fair idea about how far the prediction temperature can be stretched beyond the actual experimental region. Typically, it is rather difficult to make reasonably precise predictions at temperatures that deviate from the experimental temperature region by more than several tens of degrees.

The limited accuracy of kinetic predictions is even bigger problem than the limited precision. This is because the accuracy cannot be evaluated without performing actual measurements under the conditions to which the prediction is made. Since kinetic predictions cannot be carried out without first making some kinetic assumption, the resulting predictions are always as accurate as the underlying assumption made to carry them out. As already mentioned, the underlying assumption of kinetic predictions is that the rate equations and respective kinetic triplets evaluated within an experimental range of temperatures would remain the same outside this range. Extensive experience suggests that most of the time such assumption is fairly accurate at least when the temperature range of the predictions does not extend more than several tens of degrees beyond the experimental range. However, this should not be taken as a rule because sometimes even very small temperature can cause a failure of the underlying assumption. An example of such situation is when the temperature regions of experiment and prediction are separated by a phase transition. As discussed in Sect. 1.3, the kinetic triplets may change significantly due to melting [83] or solid–solid phase transitions [84, 85]. In particular, one should be extremely cautious when trying to predict the thermal stability of a solid material from higher temperature data obtained above the melting temperature of the solid material.

Another implicit assumption that may affect the accuracy of kinetic predictions is that a process proceeds to completion, i.e.,  $\alpha$  changes from 0 to 1, regardless of the heating rate and/or temperature. This is not always the case. A well-known example is the reaction of epoxy curing. At higher temperatures and/or faster heating rates, the reaction proceeds to completion (i.e.,  $\alpha = 1$ ), yielding a fully cured epoxy material that is characterized by the limiting glass transition temperature. If curing is performed isothermally below the limiting glass transition temperature, the reaction system vitrifies effectively, stopping the process. The resulting material reaches some ultimate extent of cure that is smaller than 1 (i.e.,  $\alpha < 1$ ). The use of progressively lower curing temperatures results in progressively smaller ultimate extents of cure. Then, the use of complete cure data for predicting the curing below the limiting glass transition temperature would result in inaccurate predictions, with the ultimate extent of cure equal to 1 as shown in Fig. 2.20 [86]. Elimination of the inaccuracy requires introduction of a diffusion correction factor that accounts for vitrification [86].

Yet another source of inaccuracy in kinetic predictions is linked to the inaccuracy of determining  $\alpha = 0$ . This is easy to understand upon recognizing that Eq. 2.39 takes its origin from Eq. 2.6, in which the lower limit of integration is 0. This means that Eq. 2.39 assumes that the process starts when  $t$  and  $\alpha$  are zero. However, for all practical purposes, the process starts when it becomes detectable experimentally.

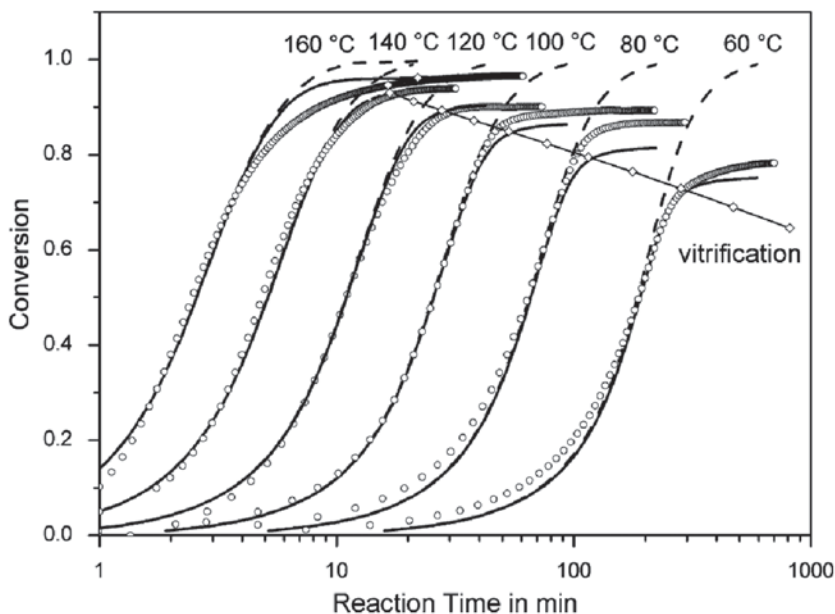


**Fig. 2.20** Model-free predictions (*dash lines*) of epoxy-amine curing reaction at a series of temperatures from 60 to 160 °C. *Dots* represent the actually measured data. *Solid lines* are predictions corrected for vitrification. (Reproduced from Schawe [86] with permission of Elsevier)

This happens when  $\alpha$  reaches the detection limit,  $\alpha_0$ . This obviously occurs at a non-zero value of the time,  $t_0$ . Therefore, accepting the  $\alpha_0$  and  $t_0$  values as being negligibly different from zero introduces some systematic error into Eq. 2.39. As a result, the lifetimes predicted by Eq. 2.39 are underestimated by the actual value of  $t_0$ :

$$t_0 = \frac{g(\alpha_0)}{k(T)}. \quad (2.50)$$

Equation 2.50 indicates that the error depends on the type of  $g(\alpha)$ . As seen from Fig. 2.12, in the vicinity of  $\alpha_0 \approx 0$ , the value of  $g(\alpha_0)$  is vanishingly small for some models (e.g., diffusion and contracting geometry type) but relatively large for others (e.g., Avrami–Eroffev and power law models). This means that the assumption that  $\alpha_0$  and  $t_0$  being zero would introduce negligible errors for the first type of the models but may result in significant error for the second kind of the models. Recall that the models of the first type belong to the class of decelerating models (see Sect. 1.1, Fig. 1.5). They represent processes whose rate under isothermal conditions is the fastest at  $\alpha=0$ . For this reason, the process tends to become detectable at negligibly small values of  $t_0$ .

The second type of models is from the class of either accelerating or sigmoid models. Under isothermal conditions, the respective processes have the slowest rate at  $\alpha=0$  (Fig. 1.5). More importantly, these models represent the processes that tend to have an induction period. In this case, the process may become detectable when



$t_0$  is much larger than zero. Therefore, when an isothermal experiment identifies a process as belonging to this type, one should be mindful of making predictions especially to lower temperatures. This is because, as per Eq. 2.50, the systematic error increases exponentially with decreasing temperature.

## References

1. Kujirai T, Akahira T (1925) Effect of temperature on the deterioration of fibrous insulating materials. *Sci Papers Inst Phys Chem Res Tokyo* 2:223–252
2. Vyazovkin S (2000) Kinetic concepts of thermally stimulated reactions in solids: a view from a historical perspective. *Int Rev Phys Chem* 19:45–60
3. Dakin TW (1948) Electrical insulation deterioration treated as chemical rate phenomenon. *AIEE Trans* 67:113–122
4. Emanuel NM, Knorre DG (1973) *Chemical kinetics (homogenous reactions)*. Wiley, New York
5. Barret P (1973) *Heterogeneous kinetics*. Gauthier-Villars, Paris (in French)
6. Rozovskii AY (1974) *Kinetics of topochemical reactions*. Chemistry. Khimiya, Moscow (in Russian)
7. Tret'yakov YuD (1978) *Solid-state reactions*. Chemistry. Khimiya, Moscow (in Russian)
8. Garner WE (ed) (1955) *Chemistry of the solid state*. Butterworth, London
9. Young DA (1966) *Decomposition of solids*. Pergamon, Oxford
10. Schmalzried H (1995) *Chemical kinetics of solids*. Wiley, Weinheim
11. Brown ME, Dollimore D, Galwey AK (1980) *Reactions in the solid state*. Elsevier, Amsterdam
12. Wendlandt WW (1986) *Thermal analysis*, 3rd edn. Wiley, New York
13. Friedman HL (1964) Kinetics of thermal degradation of char-forming plastics from thermogravimetry. Application to a phenolic plastic. *J Polym Sci Part C* 6:183–195
14. Ozawa T (1965) A new method of analyzing thermogravimetric data. *Bull Chem Soc Japan* 38:1881–1886
15. Flynn JH, Wall LA (1966) A quick, direct method for the determination of activation energy from thermogravimetric data. *J Polym Sci B Polym Lett* 4:323–328
16. Flynn JH, Wall LA (1966) General treatment of the thermogravimetry of polymers. *J Res Nat Bur Standards Part A* 70:487–523
17. Flynn JH (1997) The ‘Temperature Integral’—its use and abuse. *Thermochim Acta* 300:83–92
18. Starink MJ (2007) Activation energy determination for linear heating experiments: deviations due to neglecting the low temperature end of the temperature integral. 42:483–489
19. Doyle CD (1962) Estimating isothermal life from thermogravimetric data. *J Appl Polym Sci* 6:639–642
20. Elder JP (1984) Multiple reaction scheme modeling. I. Independent and competitive first order reactions. *J Therm Anal* 29:1327–1342
21. Elder JP (1988) Multiple reaction scheme modeling. II. Parameter selection and re-examination of mutually independent first order reactions. *J Therm Anal* 34:1467–148
22. Elder JP (1989) Multiple reaction scheme modeling. III. Mutually independent nth order reactions. *J Therm Anal* 35:1965–1984
23. Elder JP (1990) Multiple reaction scheme modeling. IV. Mutually independent random nucleation reactions. *J Therm Anal* 36:1077–1112
24. Dowdy DR (1987) Meaningful activation energies for complex systems. I. The application of the Ozawa-Flynn-Wall method to multiple reactions. *J Therm Anal* 32:137–147
25. Dowdy DR (1987) Meaningful activation energies for complex systems. II. Evaluation of the Friedman method when applied to multiple reactions, and comparison with the Ozawa-Flynn-Wall method. *J Therm Anal* 32:1177–1187

26. Vyazovkin SV (1993) An approach to the solution of the inverse kinetic problems in the case of complex reactions. IV. Chemical reaction complicated by diffusion. *Thermochim Acta* 223:201–206
27. Vyazovkin SV (1994) Conversion dependence of activation energy for model DSC curves of consecutive reactions. *Thermochim Acta* 236:1–13
28. Vyazovkin S, Linert W (1995) Kinetic analysis of reversible thermal decomposition of solids. *Int J Chem Kinet* 27:73–84
29. Vyazovkin S (1996) A unified approach to kinetic processing of nonisothermal data. *Int J Chem Kinet* 28:95–101
30. Flynn JH (1983) The isoconversional method for determination of energy of activation at constant heating rates. *J Therm Anal* 27:95–102
31. Sbirrazzuoli N, Girault Y, Elégant L (1997) Simulations for evaluation of kinetic methods in differential scanning calorimetry. Part 3—peak maximum evolution methods and isoconversional methods. *Thermochim Acta* 293:25–37
32. Starink MJ (2003) The determination of activation energy from linear heating rate experiments: a comparison of the accuracy of isoconversion methods, *Thermochim Acta* 404:163–176
33. Akahira T, Sunose T (1971) Method of determining activation deterioration constant of electrical insulating materials. *Res Report Chiba Inst Technol (Sci Technol)* 16:22–31
34. Vyazovkin S, Dollimore D (1996) Linear and nonlinear procedures in isoconversional computations of the activation energy of thermally induced reactions in solids. *J Chem Inf Comp Sci* 36:42–45
35. Vyazovkin S (1997) Evaluation of the activation energy of thermally stimulated solid-state reactions under an arbitrary variation of the temperature. *J Comput Chem* 18:393–402
36. Vyazovkin S (2001) Modification of the integral isoconversional method to account for variation in the activation energy. *J Comput Chem* 22:178–183
37. Vyazovkin S, Burnham A K, Criado JM, Pérez-Maqueda LA, Popescu C, Sbirrazzuoli N (2011) ICTAC Kinetics committee recommendations for performing kinetic computations on thermal analysis data. *Thermochim Acta* 520:1–19
38. Budrugaec P (2002) Differential non-linear isoconversional procedure for evaluating the activation energy of non-isothermal reactions. *J Therm Anal Calorim* 68:131–139
39. Popescu C (1996) Integral method to analyze the kinetics of heterogeneous reactions under non-isothermal conditions. A variant on the Ozawa-Flynn-Wall method. *Thermochim Acta* 285:309–323
40. Simon P, Thomas PS, Okuliar J, Ray AS (2003) An incremental integral isoconversional method. Determination of activation parameters. *J Therm Anal Calorim* 72:867–874
41. Tang W, Chen D (2005) An integral method to determine variation in activation energy with extent of conversion. *Thermochim Acta* 433:72–76
42. Ortega A (2008) A simple and precise linear integral method for isoconversional data. *Thermochim Acta* 474:81–86
43. Cai J, Chen S (2009) New iterative linear integral isoconversional method for the determination of the activation energy varying with the conversion degree. *J Comput Chem* 30:1986–1991
44. Budrugaec P (2010) An iterative model-free method to determine the activation energy of non-isothermal heterogeneous processes. *Thermochim Acta* 511:8–16
45. Budrugaec P (2011) An iterative model-free method to determine the activation energy of heterogeneous processes under arbitrary temperature programs. *Thermochim Acta* 523:84–89
46. Han Y, Chen H, Li N (2011) New incremental isoconversional method for kinetic analysis of solid thermal decomposition. *J Therm Anal Calorim* 104:679–683
47. Han Y, Li T, Saito K (2013) A modified Ortega method to evaluate the activation energies of solid state reactions. *J Therm Anal Calorim* 112:683–687
48. Vyazovkin S, Sbirrazzuoli N (2002) Isoconversional analysis of nonisothermal crystallization of a polymer melt. *Macromol Rapid Commun* 23:766–770

49. Vyazovkin S, Sbirrazzuoli N (2004) Isoconversional approach to evaluating the Hoffman-Lauritzen parameters ( $U^*$  and  $K_g$ ) from the overall rates of nonisothermal crystallization. *Macromol Rapid Commun* 25:733–738
50. Chen K, Vyazovkin S (2009) Temperature dependence of sol-gel conversion kinetics in gelatin-water system. *Macromol Biosci* 9:383–392
51. Farasat R, Yancey B, Vyazovkin S (2013) High temperature solid-solid transition in ammonium chloride confined to nanopores. *J Phys Chem C* 117:13713–13721
52. Vyazovkin S (2002) Is the Kissinger equation applicable to the processes that occur on cooling? *Macromol Rapid Commun* 23:771–775
53. Brown ME, Maciejewski M, Vyazovkin S, Nomen R, Sempere J, Burnham A, Opfermann J, Strey R, Anderson HL, Kemmler A, Keuleers R, Janssens J, Desseyn HO, Li CR, Tang TB, Roduit B, Malek J, Mitsuhashi T (2000) Computational aspects of kinetic analysis. Part A: the ICTAC kinetics project-data, methods and results. *Thermochim Acta* 355:125–143
54. Maciejewski M (2000) Computational aspects of kinetic analysis. Part B: the ICTAC kinetics project—the decomposition kinetics of calcium carbonate revisited, or some tips on survival in the kinetic minefield. *Thermochim Acta* 355:145–154
55. Vyazovkin S (2000) Computational aspects of kinetic analysis. Part C: the ICTAC kinetics project—the light at the end of the tunnel? *Thermochim Acta* 355:155–163
56. Burnham AK (2000) Computational aspects of kinetic analysis. Part D: the ICTAC kinetics project—multi-thermal-history model-fitting methods and their relation to isoconversional methods. *Thermochim Acta* 355:165–170
57. Vyazovkin SV, Lesnikovich AI (1988) Estimation of the pre-exponential factor in the isoconversional calculation of the effective kinetic parameters. *Thermochim Acta* 128:297–300
58. Vyazovkin S, Linert W (1995) False isokinetic relationships found in the nonisothermal decomposition of solids. *Chem Phys* 193:109–118
59. Sbirrazzuoli N (2013) Determination of pre-exponential factors and of the mathematical functions  $f(\alpha)$  or  $G(\alpha)$  that describe the reaction mechanism in a model-free way. *Thermochim Acta* 564:59–69
60. Vyazovkin S, Linert W (1995) Thermally induced reactions of solids: isokinetic relationships of nonisothermal systems. *Int Rev Phys Chem* 14:355–369
61. Lesnikovich AI, Levchik SV (1983) A method of finding invariant values of kinetic parameters. *J Therm Anal* 27:89–93
62. Tang W, Liu Y, Zhang H, Wang C (2003) New approximate formula for Arrhenius temperature integral. *Thermochim Acta* 408:39–43
63. Vyazovkin SV (1992) Alternative description of process kinetics. *Thermochim Acta* 211:181–187
64. Zhou D, Schmitt EA, Zhang GGZ, Law D, Wight CA, Vyazovkin S, Grant DJW (2003) Model-free treatment of the dehydration kinetics of nedocromil sodium trihydrate. *J Pharm Sci* 92:1367–1376
65. Sestak J, Berggren G (1971) Study of the kinetics of the mechanism of solid-state reactions at increased temperature. *Thermochim Acta* 3:1–12
66. Akulov NS (1940) Basic of chemical dynamics. Moscow State University, Moscow. (in Russian)
67. Young DA (1966) Decompositions of solids. Pergamon, Oxford
68. Perez-Maqueda LA, Criado JM, Sanchez-Jimenez PE (2006) Combined kinetic analysis of solid-state reactions: a powerful tool for the simultaneous determination of kinetic parameters and the kinetic model without previous assumptions on the reaction mechanism. *J Phys Chem A* 110:12456–12462
69. Malek J (1992) The kinetic-analysis of nonisothermal data. *Thermochim Acta* 200:257–269
70. Malek J (1995) The applicability of Johnson-Mehl-Avrami model in the thermal analysis of the crystallization kinetics of glasses. *Thermochim Acta* 267:61–73
71. Criado JM, Malek J, Ortega A (1989) Applicability of the master plots in kinetic-analysis of non-isothermal data. *Thermochim Acta* 147:377–385

72. Jankovic B, Mentus S, Jelic D (2009) A kinetic study of non-isothermal decomposition process of anhydrous nickel nitrate under air atmosphere. *Physica B* 404:2263–2269
73. Vyazovkin S, Wight CA (1999) Model-free and model-fitting approaches to kinetic analysis of isothermal and nonisothermal data. *Thermochim Acta* 340–341:53–68
74. ASTM E1641-07 (2007) Standard test method for decomposition kinetics by thermogravimetry, Annual book of ASTM standards, vol 14.02, ASTM International, West Conshohocken
75. ASTM E698-05 (2005) Standard test method for Arrhenius kinetic constants for thermally unstable materials, Annual book of ASTM standards, vol 14.02, ASTM International, West Conshohocken
76. Kissinger HE (1956) Variation of peak temperature with heating rate in differential thermal analysis. *J Res Natl Bur Stand* 57:217–221
77. Kissinger HE (1957) Reaction kinetics in differential thermal analysis. *Anal Chem* 29:1702–1706
78. Prime RB, Bair HE, Vyazovkin S, Gallagher PK, Riga A (2009) Thermogravimetric analysis. In: Menczel JD, Prime RB (eds) *Thermal analysis of polymers, fundamentals and applications*. Wiley, New York, pp 241–317
79. Vyazovkin S, Sbirrazzuoli N (1996) Mechanism and kinetics of epoxy-amine cure studied by differential scanning calorimetry. *Macromolecules* 29:1867–1873
80. Vyazovkin SV, Lesnikovich AI (1988) Transformation of “degree of conversion against temperature” into “degree of conversion against time” kinetic data. *Russ J Phys Chem* 62:1535–1537
81. Vyazovkin S, Dranca I, Fan X, Advincula R (2004) Kinetics of thermal and thermo-oxidative degradation of polystyrene clay nanocomposite. *Macromol Rapid Commun* 25:498–503
82. Vyazovkin S, Linert W (1994) Reliability of conversion—time dependencies as predicted from thermal analysis data. *Anal Chim Acta* 295:101–107
83. Bawn CEH (1955) Decomposition of organic solids. In: Garner WE (ed) *Chemistry of the solid state*. Butterworth, London, pp 254–267
84. Hedvall JA (1934) Changes in crystal structure and their influence on the reactivity and catalytic effect of solids. *Chem Rev* 15:139–168
85. Gallagher PK, Sanders JP (2003) Ceramics, glass, and electronic materials. In: Brown ME, Gallagher PK (eds) *The handbook of thermal analysis & calorimetry. Applications to inorganic and miscellaneous materials*, vol 2. Elsevier, Amsterdam, pp 191–260
86. Schawe JEK (2002) A description of chemical and diffusion control in isothermal kinetics of cure kinetics. *Thermochim Acta* 388:299–312

Isoconversional Kinetics of Thermally Stimulated  
Processes

Vyazovkin, S.

2015, XIII, 239 p. 165 illus., 6 illus. in color., Hardcover

ISBN: 978-3-319-14174-9